



Insights into nonlinear adsorption kinetics and isotherms of vanadium using magnetised coal-polyaniline

George William Kajjumba^a, Eren Yildirim^b, Faisal Osra^c, Serdar Aydin^{d,*},
Tran Thi Kieu Ngan^e, Serkan Emik^{b,*}

^aDepartment of Civil and Environmental Engineering and Construction, University of Nevada, Las Vegas, USA,
email: gwkajjumba@gmail.com

^bDepartment of Chemical Engineering, Istanbul University-Cerrahpaşa, Istanbul, Turkey, emails: s.emik@istanbul.edu.tr (S. Emik),
aramiseren@gmail.com (E. Yildirim)

^cDepartment of Civil Engineering, Umm Alqura University, Makkah, Saudi Arabia, email: faisalosra@gmail.com

^dDepartment of Environmental Engineering, Istanbul University-Cerrahpaşa, Istanbul, Turkey, email: saydin@istanbul.edu.tr

^eFaculty of Environmental and Chemical Engineering, Duy Tan University, Da Nang, Vietnam, email: trankieungan5885@gmail.com

Received 8 May 2019; Accepted 26 September 2019

ABSTRACT

Remediation of the polluted environment has become a major concern in the 21st century. Because of its cost-benefit, ease of application, and efficacy towards the removal of pollutants, the adsorption technique has gained acceptance. In this study, adsorption kinetics of vanadium onto magnetized coal-polyaniline (MC-PANI) are investigated under batch experiments. Isotherms and kinetics are assessed using average relative error deviation, Marquardt's percent standard error deviation, the hybrid fractional error function, chi-square (χ^2), Spearman, and the sum of the squares of the errors (SSE). Comparing all of the error functions, nonlinear models explain the adsorption of vanadium better than linear models. According to the Boyd model, the adsorption of vanadium occurs in two stages. The maximum adsorption capacity of MC-PANI is 66.20 mg V/g ($C_0 = 50$ mg/L, pH = 5, dose = 1.5 g/L, $T = 25^\circ\text{C}$). Based on Freundlich's dimensionless constant, which determines the driving force of adsorption, adsorption was less favored during the adsorption of vanadium; both amine and Fe_3O_4 participated in the removal of vanadium through ligand or ion exchange.

Keywords: Error function; Conducting polymers; Batch adsorption; Wastewater; Polymerization

1. Introduction

Freshwater availability will be the most challenging problem in the mid-21st century. Improved standards of living and industrialization have led to the increased consumption and extraction of natural minerals. Among these minerals are rare metals whose effects on humans are still unknown; however, the available studies indicate that some of these metals are dangerous even at micro levels in the water. Vanadium is a rare earth metal whose levels have been reported to be increasing in water in different parts of the

world. The consumption of vanadium contaminated substances (1.0 mg/L) has been reported to cause a diverse effect on avian, aquatic, and human life [1,2].

However, removing vanadium from a solution is a challenge. Different processes have been developed [3,4], but the adsorption process is a promising mechanism towards the extraction of rare metals from wastewater [5–7]. Before applying the adsorption technique, the influential kinetic and isotherm parameters must be investigated to optimize the adsorption process, adsorbate–adsorbent interaction,

* Corresponding authors.

reaction pathway, rate of adsorption, and adsorption mechanism. Some studies have examined the removal of vanadium from wastewater, and a Langmuir isotherm and second-order (SO) kinetics have been favored. However, the parameters are only based on linearised forms of adsorption kinetics and isotherms.

Basing adsorption parameters on linearised forms of first-order (FO) and SO kinetics, as well as Langmuir and Freundlich isotherms, are extremely misleading during the design of the actual adsorption system. Nonlinear forms of both kinetics and isotherms have been proved to be accurate over linearised forms. To choose the best kinetic or isotherm that controls the adsorption process, error functions are assessed. For instance, during the assessment of linear FO, $\ln(q_i - q_e)$ is plotted against time. As the system approaches equilibrium, the fitting index is reduced since $\ln(q_e - q_i)$ becomes extremely large. Different forms of linear SO have been developed to estimate the kinetic parameters with [8]'s model being the most prominent.

The dependent variables are not entirely linear over the given values of the independent variable in isotherm equations. The inverse of data weights ($1/q_e$) and the presence of an independent variable (C_e) in both dependent and independent sides cause false correlation. The inverting of variables on both sides in some isotherm equations distorts the error distribution over the entire data. In some forms of Langmuir, the presence of a dependent parameter (q_e) on both sides leads to a spurious correlation. R^2 is a very sensitive parameter that can cause spurious conclusions. R^2 varies with the range of the independent parameter: if the range is big, R^2 will fit; and if the range is small, fit will be poor. Adding more data points decreases the degree of freedom of a system, which favors the model fit. Making conclusions solely based on R^2 can be misleading during industrial applications.

Therefore, this study assesses the applicability of linear and nonlinear adsorption kinetics and isotherms during the removal of vanadium by magnetized coal-polyaniline (MC-PANI). Hypothesis: nonlinear kinetics explain adsorption better than linear kinetics.

2. Materials and methods

2.1. Chemicals

For this study, coal was mined from Trakya, Turkey (GPS: 41.141968N, 28.353888E). Iron(III) chloride ($\text{FeCl}_3 \cdot 6\text{H}_2\text{O}$, 98%–102%), iron(II) chloride ($\text{FeCl}_2 \cdot 4\text{H}_2\text{O}$, 99%), and ammonium hydroxide (NH_4OH , 26%) were used in the synthesis of magnetic particles. Aniline ($\text{C}_6\text{H}_5\text{NH}_2$), ammonium persulfate ($(\text{NH}_4)_2\text{S}_2\text{O}_8$, 98%) and hydrochloric acid (HCl, 37%) were used to generate a polyaniline structure. NH_4VO_3 was expended to prepare a standard vanadium solution. All chemicals were supplied by Merck chemicals (Darmstadt, Germany). Deionized water was used in all the experiments.

2.2. MC-PANI synthesis and characterization

2.2.1. Magnetic coal

The coal was cleaned with deionized water and then dried for 36 h. The dried materials were then conditioned

using 1 M NaCl for 24 h. they were then sieved and rewashed with deionized water, and dried for 36 h. To produce magnetic coal, 75 ml of 0.15 M $\text{FeCl}_2 \cdot 4\text{H}_2\text{O}$ (1.71 g) and 150 ml of 0.15 M $\text{FeCl}_3 \cdot 6\text{H}_2\text{O}$ (3.65 g) were mixed with 3 g of coal for 30 min at 80°C in a conical flask under a nitrogen atmosphere. Afterward, 50 ml of 2 M NH_4OH were added rapidly to adjust the pH to about 10 [9]. The temperature of the resultant mixture was maintained at 80°C for 1 h. The formed magnetic coal was collected by an external magnet, cleaned with deionized water, and dried under vacuum for 24 h.

2.2.2. Magnetised coal polyaniline

For the MC-PANI, 2.7 ml of aniline solution was mixed with 50 ml of 0.1 M HCl for 20 min at a temperature below 5°C; then 3.0 g of magnetized coal was added and stirred vigorously for 10 min. For polymerization, 8.55 g $(\text{NH}_4)_2\text{S}_2\text{O}_8$ were mixed with 50 ml of 0.1 M HCl, then added slowly; the resultant mixture was stirred for 5 h. To the resultant mixture, 50 ml of 1 M NH_4OH were added (to neutralize), and the system was left to age for 36 h [9]. The solution was filtered with the help of an external magnet, and the formed MC-PANI was washed with deionized water until a neutral pH was attained; then it was dried in vacuum for 24 h. 4.4 g of MC-PANI were synthesized.

2.3. Characterization

The Burker Alpha-P (USA) Fourier-transform infrared (FTIR) spectra were utilized to study the structure of the MC-PANI before and after adsorption. A thermogravimetric analyzer (model: LINSEIS STA PT1750, Germany) was used to analyze the amount of Fe_3O_4 and polyaniline formed on the coal and the thermal behavior, while X-ray Diffraction (XRD) and scanning electron microscopy (SEM) (model, JEOL/JSM-6610, Japan) were used to study the morphology of the coal.

2.4. General batch adsorption studies

The standard vanadium solution was prepared by dissolving NH_4VO_3 in deionized water. Adsorption batch studies were assessed by agitating 0.03 g of MC-PANI with 20 ml of vanadium solution (10–100 mg/L) for 24 h at 140 rpm. Thermodynamic parameters were examined by adjusting the temperature between 10°C and 40°C. The pH effect was studied by adjusting the pH from 2.0 to 11 by adding negligible volumes of HCl and NaOH. After adsorption, the adsorbent was separated using an external magnet. Then the solution was filtered and analyzed to determine the residual vanadium using the Gallic acid method [10]; the equilibrium was examined with Eq. (1) [11,12]:

$$q_e = \frac{(C_0 - C_e)}{m} \times V \quad (1)$$

where C_0 is the initial concentration of vanadium (mg/L), C_e is the equilibrium concentration (mg/L), q_e is the equilibrium amount of vanadium adsorbed (mg/g), m is the adsorbent's mass (g), and V is the volume solution.

2.5. Validity of adsorption kinetic and isotherm models

Apart from R^2 , the suitability of the models was validated with normalized standard deviation (NSD), average relative error (ARE), Marquardt's percent standard deviation (MPSD), sum squares errors (SSE), hybrid error function (HYBRID), Spearman's correlation coefficient (r_s), and non-linear chi-square tests (χ^2), as defined in Table 1 [13,14]. where q_{exp} is observed from the batch experiment, q_{cal} is estimated from the model, n is the number of observations in the experiment, and p is the number of parameters in the regression model.

3. Results and discussion

3.1. Characterization

The preparation and characterization of MC-PANI have been already published [9]. Briefly, according to XRD analysis, the main components of the coal were found to be kaolinite, quartz, goethite, and gibbsite and the polymerization of MC increased the amorphous nature of the adsorbent, which is good for adsorption. A close assessment of SEM images showed that polyaniline formed a spiral network around the magnetized coal; thus, the successful formation of MC-PANI and the thermogravimetric analysis indicated that the amount of PANI in MC-PANI adsorbent was 42% (w). In the comparison of the FTIR spectrum (Figs. 1a and b), the shift of 512 peak coal to 509, and its reduction in intensity indicate the formation of Fe_3O_4 in the matrix [9]. The incipient

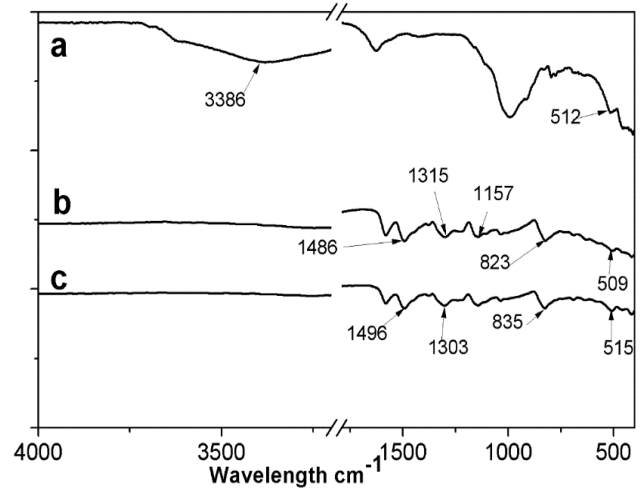


Fig. 1. FTIR spectrum of (a) coal, (b) MC-PANI, and (c) after vanadium adsorption.

peaks at 1,486; 1,315; and 1,157 cm^{-1} (Fig. 1b) correspond to tertiary dimethyl amines ($-\text{N}(\text{CH}_3)_2$) rocking vibrations [15].

3.2. pH study

pH is an important parameter that determines the interaction between the adsorbent and the adsorbate. It not only affects the adsorbents' charge in solution but also the adsorbate's charge. The pH effect was studied by mixing 1.5 g/L of the adsorbent with 20 ml of 50 mg/L of vanadium solution at different pHs, between 2.0 and 11.0. Fig. 2 shows the sorption of vanadium; from the speciation analysis of vanadium at $\text{pH} \leq 3.0$, the major form of vanadium is pentavalent cation VO_2^+ , while at $3.0 < \text{pH} < 5.0$, pentavalent anions, VO_3^- are the major species of vanadium in the solution [6]. Therefore, an increase in adsorption capacity ($\text{pH} \geq 3.0$) is attributed to the electrostatic attraction between VO_3^- and the amine functional group on polyaniline. The slight decrease in adsorption capacity of vanadium by MC-PANI at $\text{pH} > 8$ is attributed both to the decreased positive charged of the adsorbent surfaces and the formation of vanadium polymers that have less removal efficiency.

3.3. Adsorption kinetics

According to Fig. 3, the adsorption capacity increased with time until the equilibrium was attained, when there was barely any increase in the adsorption capacity. Most of the vanadium ions were removed within 90 min (more than 75%). The adsorption kinetics of vanadium by activated coal was studied with FO and SO kinetics. Linear and nonlinear kinetics are summarized in Table 2 [8,16,17]; the parameters and error values of each equation are summarized in Table 3.

As the general rule of using R^2 as a measure of fitness, the linearised form of kinetics, SO I is favored during the adsorption of vanadium. Although linearised R^2 favors SO I, assessment of other error functions of SE, χ^2 , NSD, r_s , MPSD,

Table 1
Error functions

NSD	$100 \sqrt{\frac{1}{n-1} \sum_{i=1}^n \left[\frac{q_{\text{exp}} - q_{\text{cal}}}{q_{\text{exp}}} \right]^2}$
ARE	$\frac{100}{n} \sum_{i=1}^n \left \frac{q_{\text{exp}} - q_{\text{cal}}}{q_{\text{exp}}} \right $
MPSD	$100 \sqrt{\frac{1}{n-p} \sum_{i=1}^n \left[\frac{q_{\text{exp}} - q_{\text{cal}}}{q_{\text{exp}}} \right]^2}$
SSE	$\sum_{i=1}^n [q_{\text{exp}} - q_{\text{cal}}]_i^2$
HYBRID	$\frac{100}{n-p} \sum_{i=1}^n \left[\frac{(q_{\text{exp}} - q_{\text{cal}})^2}{q_{\text{exp}}} \right]_i$
r_s	$1 - \frac{6 \sum_{i=1}^n [q_{\text{exp}} - q_{\text{cal}}]_i^2}{n(n^2 - 1)}$
χ^2	$\sum_{i=1}^n \left[\frac{(q_{\text{exp}} - q_{\text{cal}})^2}{q_{\text{exp}}} \right]_i$

and HYBRID favor SO III. Based on calculated q_{cal} , SO IV shows that q_{cal} is close to the experimental value. Comparing the variation of linear SO models and a nonlinear SO model, there is little variation between SO III and a nonlinear model. Therefore, a SO III linear model is more accurate in predicting adsorption kinetics than any other linearized model. Fig. 3 shows the nonlinear adsorption kinetics of vanadium. Assessment of kinetics using nonlinear models still favors SO. Comparing the linear and nonlinear forms of FO shows a great improvement in the model fit when nonlinear kinetics are expended. The R^2 of FO improved by over seven points (0.890 vs. 0.962). Comparing the correlation coefficient of linear FO kinetics in the literature [7,18] with the nonlinear R^2 of this study shows a greater improvement of the model fit. Therefore, before any conclusions are made regarding adsorption kinetics, both linear and nonlinear models should be investigated.

3.4. Diffusion mechanism

Under proper and vigorous mixing, the rate-limiting step of adsorption is intra-particle (IP) diffusion rather than mass transfer. When the plot of q_t vs. \sqrt{t} is linear ($R^2 \geq 0.95$), IP is the limiting step, while the intercept indicates the effect of the boundary layer effect. However, during the adsorption of ions, the plot of q_t vs. \sqrt{t} is not always linear over the entire time scale. The segments are related to (i) bulk transfer, which occurs at the initial stage and is very fast; thus, it is not considered in the design of the adsorption engineering process, (ii) film diffusion where the adsorbate reaches the external surface of the adsorbent is relatively slow, and (iii) the third segment is IP diffusion, which is a very slow process involving solute movement to the internal pores of the adsorbent [9].

The diffusion of vanadium by MC-PANI (Fig. 4) shows a two-segmented graph; the adsorption of vanadium is not entirely controlled by IP diffusion. The first segment is attributed to fast adsorption (film diffusion) of vanadium, followed by IP as the rate-limiting step.

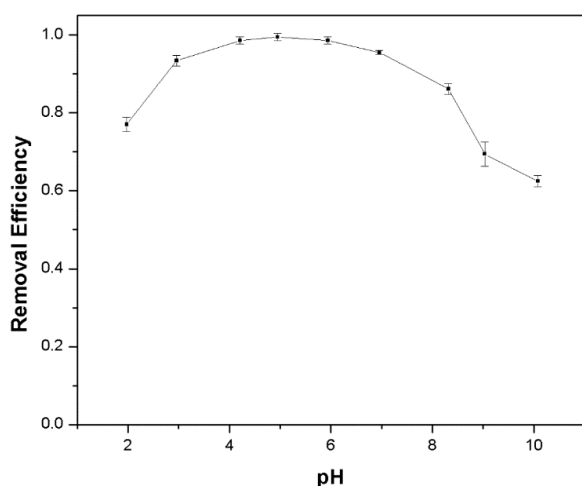


Fig. 2. Effect of pH on vanadium adsorption by MC-PANI.

To further confirm the rate-limiting step, the Fourier model was applied using Eqs. (2)–(5) [19].

$$F = 1 - \frac{6}{\pi^2} \sum_{n=1}^{\infty} \left(\frac{1}{n^2} \right) \exp(-n^2 B_t) \quad (2)$$

$$F = \frac{q_t}{q_{\infty}} \quad (3)$$

$$0 \leq F \leq 0.85: B_t = 2\pi - \frac{\pi^2 F}{3} - 2\pi \left(1 - \frac{\pi F}{3} \right)^{\frac{1}{2}} \quad (4)$$

$$0.86 \leq F \leq 1: B_t = -0.4977 - \ln(1 - F) \quad (5)$$

where F is an adsorbed fraction of adsorbate at time t (q_t) to adsorbate adsorbed at an infinite time (q_{∞}) ($t_{\infty} = 48\text{h}$); B_t is a Fourier function of F , and B_t is estimated using an integrated Fourier transform of Eqs. (4) and (5); when the graph of B_t vs. t approximate $y = mx$ line, the rate-limiting step is IP; otherwise, film diffusion controls the process. Fig. 5 shows the plot of B_t vs. t ; the intercept is not zero, and thus, the film diffusion had a greater effect during the adsorption of vanadium. This can be attributed to the fact that during the stirring of the adsorbent in the vanadium solution, the centrifugal force pushed the adsorbent particles away from the center of the flask. This creates an improper distribution of the adsorbent in the solution.

3.5. Equilibrium isotherms

An isotherm is a curve or a line describing the retention or release of a substance from an aqueous environment to a solid-phase at a given temperature, concentration, and pH. The ratio between the adsorbed and non-adsorbed vanadium (adsorption equilibrium: adsorption and desorption rates are equal) was established by contacting 10–100 mg/L V for 24 h. To understand the vanadium-solid phase, as

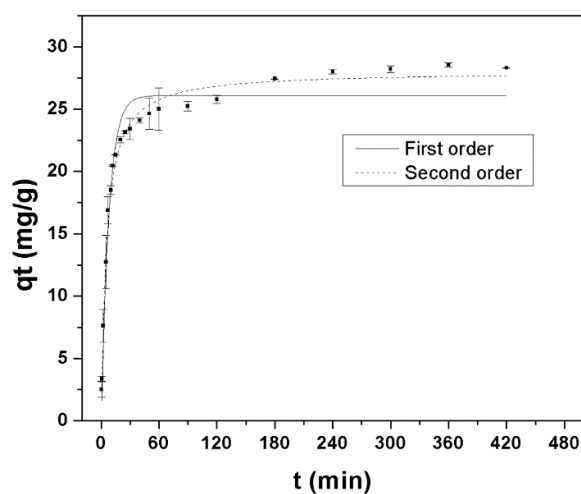


Fig. 3. Nonlinear adsorption kinetics of vanadium ($C_0 = 50$ mg/L and Dose = 1.5 g/L).

Table 2
Linear and nonlinear kinetic models

Model	Nonlinear	Linearized	Plot
FO	$q_t = q_e (1 - e^{-k_1 t})$	$\ln(q_e - q_t) = \ln(q_e) - k_1 t$	$\ln(q_e - q_t)$ vs. t
SO	$q_t = \frac{q_e^2 k_2 t}{1 + q_e k_2 t}$	SO I: $\frac{t}{q_t} = \frac{t}{q_e} + \frac{1}{k_2 q_e^2}$	$\frac{t}{q_t}$ vs. t
		SO II: $\frac{1}{q_t} = \frac{1}{q_e} + \frac{1}{k_2 q_e^2 t}$	$\frac{1}{q_t}$ vs. $\frac{1}{t}$
		SO III: $q_t = q_e - \frac{q_t}{k_2 q_e^2 t}$	q_t vs. $\frac{q_t}{t}$
		SO IV: $\frac{q_t}{t} = k_2 q_e^2 - k_2 q_e q_t$	$\frac{q_t}{t}$ vs. q_t

Table 3
Kinetic parameters of vanadium adsorption by MC-PANI at 50 mg/L, pH 5.0, dose of 1.5 g/L

	q_{exp}	q_{cal}	k	SSE	χ^2	ARE	NSD	r_s	MPSD	HYBRID	R^2
Nonlinear parameters											
FO	32.70	26.10	0.127	45.49	2.42	7.92	11.37	0.970	11.66	12.72	0.962
SO	32.70	28.03	0.007	10.75	0.78	4.29	7.93	0.993	8.14	4.13	0.991
Linear kinetic parameters											
FO		26.37	0.049	454.23	28.69	23.69	36.46	0.705	37.40	151.02	0.890
SO I		29.33	0.006	23.59	1.19	2.88	7.53	0.985	7.73	6.26	0.991
SO II		25.64	0.008	75.26	3.26	8.43	10.13	0.951	10.40	17.18	0.963
SO III		28.77	0.006	14.85	0.87	4.46	7.33	0.990	7.52	4.60	0.905
SO IV		30.23	0.005	48.81	2.14	6.76	8.52	0.968	8.74	11.27	0.905

well as quantify and contrast the performance of MC-PANI, Langmuir and Freundlich’s isotherms were studied.

$$q_e = K_F C_e^{\frac{1}{n}} \tag{6}$$

3.6. Freundlich isotherm

The Freundlich isotherm is used to explain the heterogeneous characteristics of an adsorption surface, an interactive intensity on activated coal. However, this equation cannot explain the linearity and saturation effect at very low and high concentrations, respectively. The nonlinear, linear, and incorrect linear (Eq. 9) forms of Freundlich are shown in Eqs. (6)–(9) [20], respectively. Among the Freundlich parameters, n has been misrepresented; $n = 1$ as linear adsorption, and $n > 1$ as physical adsorption, while $n < 1$ as chemical adsorption. However, when $n = 1$, it implies a linear isotherm, which can happen at low concentration or when the system does not attain equilibrium; $n > 1$ is unfavorable adsorption and $n < 1$ is favorable adsorption. Some lab groups have suggested $n > 10$ [21]; however, it is practically impossible to obtain n values higher than 10. The value of $n > 10$, implies miscalculations; otherwise, the isotherm should be validated by plotting q_e vs. C_e on a complete isotherm.

$$\ln q_e = \frac{1}{n} \ln C_e + \ln K_F \tag{7}$$

$$\log_{10} q_e = \frac{1}{n} \log_{10} C_e + \log_{10} K_F \tag{8}$$

$$\log_{10} q_e = \frac{1}{n \log_{10} C_e} + \log_{10} K_F \tag{9}$$

where q_e (mg/g) is the equilibrium adsorption, C_e (mg/L) is the equilibrium concentration in the solution, K_F (mg/g)/(mg/L) is a constant, and n is an intensity dimensionless constant that determines the driving force of adsorption.

Linearizing the Freundlich isotherm using \log_{10} or \log_e yields the same results, Fig. 6. When comparing the nonlinear and linear parameters of the Freundlich isotherm

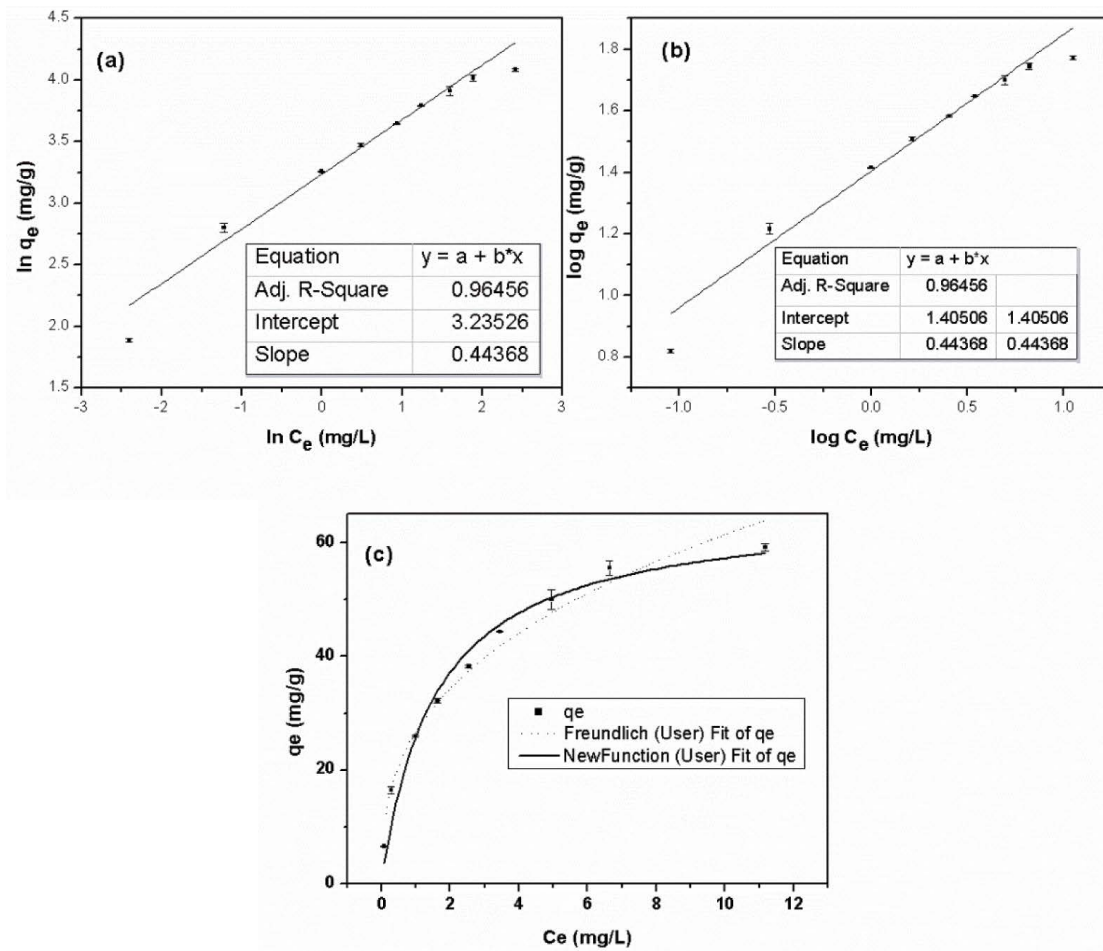


Fig. 6. Linear models of the Freundlich model based on (a) \ln , (b) \log , and (c) nonlinear Freundlich and Langmuir isotherms (pH = 5.0, $T = 25^\circ\text{C}$, Dose = 1.5 g/L).

Table 4
Statistical analysis of adsorption isotherms

	Langmuir						
	Nonlinear	Eq. (11)	Eq. (12)	Eq. (13)	Eq. (14)	Modified Eq. (13)	Modified Eq. (14)
q_m (mg/g)	66.20	65.27	50.20	54.36	84.93	67.13	22.30
b (L/mg)	0.642	0.744	1.659	1.409	1.219	0.594	0.573
R	0.973	0.989	0.993	0.846	0.846	0.957	0.957
	Freundlich						
	Nonlinear	Eq. (7)	Eq. (8)				
K_f (mg/g)/(mg/L)	26.76	24.12	24.12				
n	2.768	2.227	2.227				
R	0.971	0.964	0.964				

(Table 4), there is barely any difference; thus, both linear and nonlinear Freundlich isotherms can be used interchangeably. The values of $n > 1.0$; thus, adsorption is not the main mechanism of vanadium adsorption by MC-PANI. This is confirmed by Figs. 1b and c before and after adsorption; there is no development of a new major peak. The weakening,

disappearance, and shifting of MC-PANI peaks after adsorption confirm the adsorption of vanadium through ion or ligand exchange. For example, the Fe_3O_4 peak (509 cm^{-1}) shifted to 515 cm^{-1} , while tertiary dimethyl amines ($-\text{N}(\text{CH}_3)_2$) rocking vibration peaks of MC-PANI at $1,486$ and $1,315\text{ cm}^{-1}$ [22], shifted to $1,496$ and $1,303\text{ cm}^{-1}$.

3.7. Langmuir isotherm

The Langmuir equation is the most widely used isotherm to describe the adsorption of substances on adsorbent at equilibrium conditions. The isotherm assumes a fixed number of active sites (mono-layer) with equal energy, and no interaction between adsorbate species. The nonlinear form of Langmuir is shown in Eq. (10) [23]; there are four linearised forms of Langmuir isotherms, Eqs. (11)–(14).

$$q_e = \frac{q_m b C_e}{1 + b C_e} \tag{10}$$

$$\frac{C_e}{q_e} = \frac{C_e}{q_m} + \frac{1}{b q_m} \tag{11}$$

$$\frac{1}{q_e} = \frac{1}{b q_m C_e} + \frac{1}{q_m} \tag{12}$$

$$q_e = \frac{-q_e}{b C_e} + q_m \tag{13}$$

$$\frac{q_e}{C_e} = -b q_e + b q_m \tag{14}$$

where q_m (mg/g) is the maximum saturated monolayer adsorption capacity, C_e (mg/L) is the adsorbate concentration at equilibrium, q_e (mg/g) is the amount of adsorbate uptake at equilibrium, and b (L/mg) is a constant related to the affinity between an adsorbent and adsorbate.

Theoretically, a good adsorbate is determined by its high q_m and b (steep initial adsorption). The four linearised models are summarised in Figs. 7a–d. As discussed earlier, the linearization of the model results in error modification in the independent variables and alternation of weights placed on each data. The presence of C_e in both dependent and independent variables (Eq. (11)) gives this model a fairly-good fit (Fig. 7a); the points are evenly distributed for a wide range of concentrations. In Eq. (12) the inverse of q_e makes the model very sensitive at low value, while clustering the data points around the origin (Fig. 7b). Any large error at a lower concentration is neutralized by the large values at an extreme concentration; this makes the model have a perfect fit. Eq. (12) best suits a low concentration assessment.

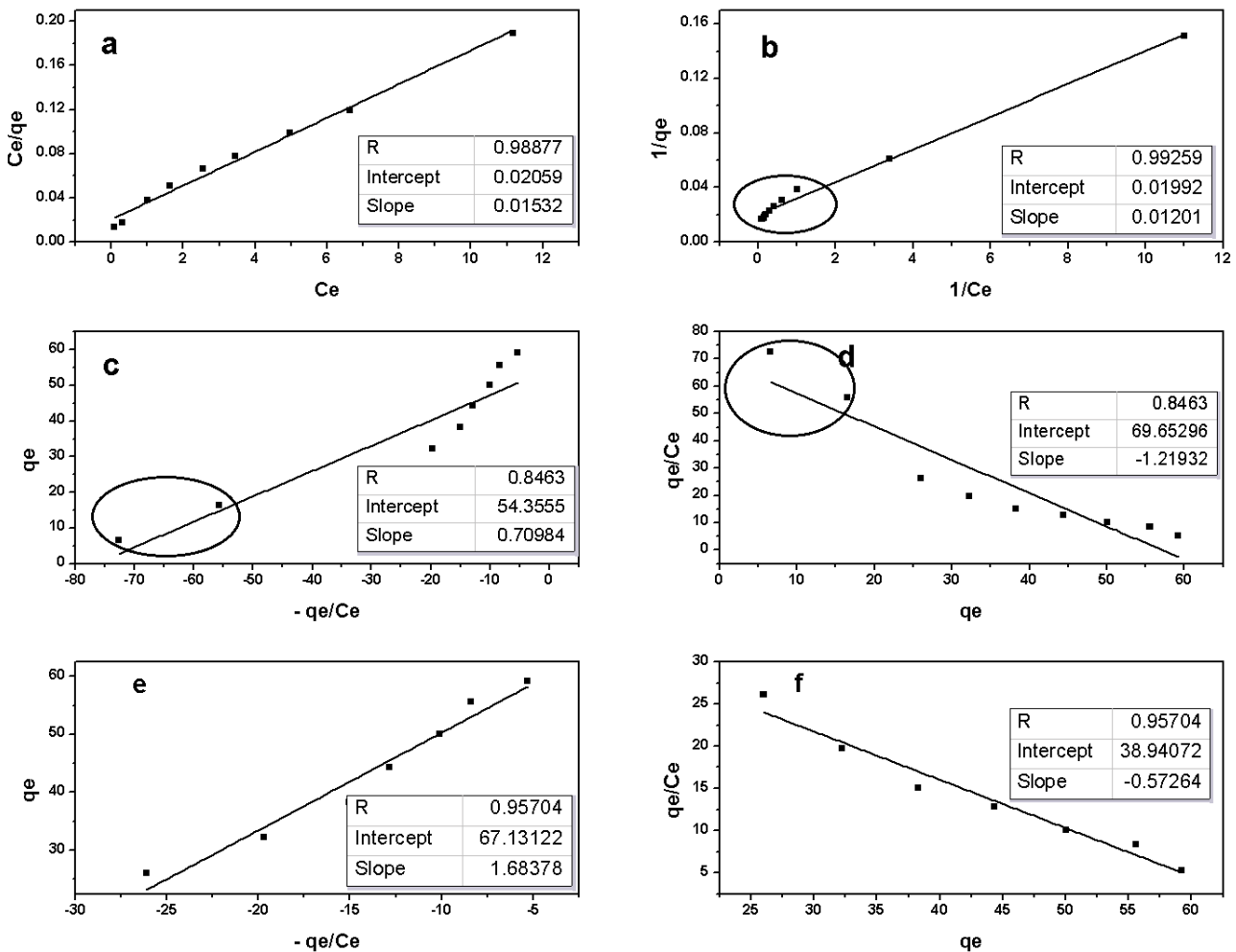


Fig. 7. Linearised form of Langmuir: (a) Eq. (11), (b) Eq. (12), (c) Eq. (13), (d) Eq. (14), (e) modified Eq. (13), and (f) modified Eq. (14) at $T = 25^\circ\text{C}$, pH 5.0, Dose = 1.5 g/L.

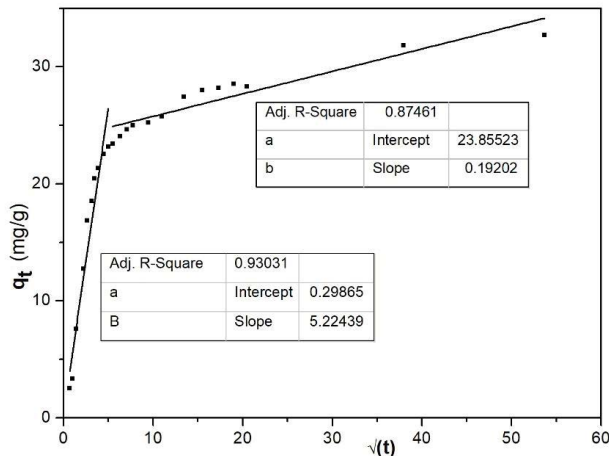
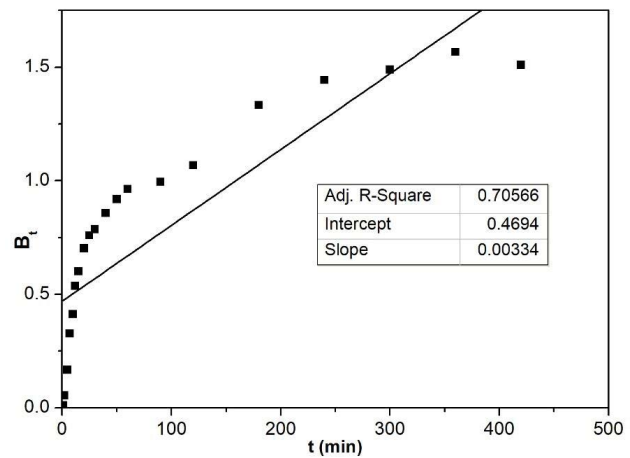
Fig. 4. Diffusion model ($C_0 = 50$ mg/L and dosage = 1.5 g/L).

Fig. 5. Boyd estimate.

Having q_e on both sides of the equation underestimates the correlation between the dependent and independent variables; this increases the error factor (Figs. 7c and d). When low concentration points are removed in both Eqs. (13) and (14), the concentration improves (Figs. 7e–f); therefore, these equations are suitable at high concentration values.

Because the nonlinear fit is the best fitting method of equilibrium isotherm, the values of q_m and b obtained by nonlinear and linearized models were compared. Table 4 shows the relative differences in the parameters of the Langmuir isotherm. As observed, Eqs. (13) and (14) produces the worst parameters when compared with the nonlinear Langmuir equation. When lower points of Eqs. (13) and (14) are deleted, both the R^2 values improve, the relative values of b are close to the nonlinear reference values.

4. Conclusion

The adsorption of vanadium by MC-PANI is very fast; over 75% of vanadium was removed within 90 min. SO kinetic model III gives little deviation from nonlinear SO; therefore, SO III is more accurate in predicting adsorption kinetics than any other linearised model. If there is a wide range of concentration, a linearised Langmuir isotherm, $\frac{C_e}{q_e} = \frac{C_e}{q_m} + \frac{1}{bq_m}$, gives better results. The adsorption of vanadium is controlled both by film diffusion (fast adsorption) and IP diffusion. At low concentrations, $\frac{1}{q_e} = \frac{1}{bq_m C_e} + \frac{1}{q_m}$ it gives better fitting, while $q_e = \frac{-q_e}{bC_e} + q_m$ and $\frac{q_e}{C_e} = -bq_e + bq_m$ are good at high concentrations. The removal of vanadium is through adsorption and ion or ligand exchange with Fe_3O_4 and $-N(CH_3)_2$. Langmuir and SO kinetics best describe the adsorption isotherm and kinetics, respectively.

References

[1] G.F. Nordberg, B.A. Fowler, M. Nordberg, Handbook on the Toxicology of Metals, 4th ed., Academic Press, Waltham, MA, USA, 2014, <https://doi.org/10.1016/C2011-0-07884-5>.

[2] M.A. Mazed, S. Mazed, Nutritional Supplement for the Prevention of Cardiovascular Disease, Alzheimer's Disease, Diabetes, and Regulation and Reduction of Blood Sugar and Insulin Resistance, US8017147B2, Patents, US, 2010.

[3] A. Keränen, T. Leiviskä, A. Salakka, J. Tanskanen, Removal of nickel and vanadium from ammoniacal industrial wastewater by ion exchange and adsorption on activated carbon, *Desal. Wat. Treat.*, 53 (2015) 2645–2654.

[4] R. Singh, A. Kumar, A. Kirrolia, R. Kumar, N. Yadav, N.R. Bishnoi, R.K. Lohchab, Removal of sulphate, COD and Cr(VI) in simulated and real wastewater by sulphate reducing bacteria enrichment in small bioreactor and FTIR study, *Bioresour. Technol.*, 102 (2011) 677–682.

[5] C. Pennesi, C. Totti, F. Beolchini, Removal of vanadium(III) and molybdenum(V) from wastewater using *Posidonia oceanica* (Tracheophyta) biomass, *PLoS One*, 8 (2013), doi: 10.1371/journal.pone.0076870.

[6] G.W. Kajjumba, S. Aydın, S. Güneysu, Adsorption isotherms and kinetics of vanadium by shale and coal waste, *Adsorpt. Sci. Technol.*, 36 (2018) 936–952.

[7] V. Doğan, S. Aydın, Vanadium(V) removal by adsorption onto activated carbon derived from starch industry waste sludge, *Sep. Sci. Technol.*, 49 (2014) 1407–1415.

[8] Y.S. Ho, G. McKay, Pseudo-second order model for sorption processes, *Process Biochem.*, 34 (1999) 451–465.

[9] G.W. Kajjumba, E. Yıldırım, S. Aydın, S. Emik, T. Ağun, F. Osra, J. Wasswa, A facile polymerisation of magnetic coal to enhanced phosphate removal from solution, *J. Environ. Manage.*, 247 (2019) 356–362.

[10] M.J. Fishman, M.W. Skougstad, Catalytic determination of vanadium in water, *Anal. Chem.*, 36 (1964) 1643–1646.

[11] S. Salehi, M. Anbia, Performance comparison of chitosan–clinoptilolite nanocomposites as adsorbents for vanadium in aqueous media, *Cellulose*, 26 (2019) 5321–5345.

[12] T.R.S. Cadaval Jr, G.L. Dotto, E.R. Seus, N. Mirlean, L.A. de Almeida Pinto, Vanadium removal from aqueous solutions by adsorption onto chitosan films, *Desal. Wat. Treat.*, 57 (2015) 16583–16591.

[13] G.W. Kajjumba, S. Emik, A. Öngen, H.K. Özcan, S. Aydın, Modelling of Adsorption Kinetic Processes—Errors, Theory and Application, In: *Advanced Sorption Process Applications*, IntechOpen, London, UK, 2018, pp. 1–9, <https://doi.org/10.5772/intechopen.80495>.

[14] A.I. Adeogun, Removal of methylene blue dye from aqueous solution using activated charcoal modified manganese ferrite ($AC-MnFe_2O_4$): kinetics, isotherms, and thermodynamics studies, *Part. Sci. Technol.*, (2019), doi:10.1080/02726351.2019.1626516.

[15] D.C. Crans, Fifteen years of dancing with vanadium, (2005), doi:10.1351/pac200577091497.

- [16] S. Lagergren, About the theory of so-called adsorption of soluble substance, *Kungliga Svenska Vetenskapsakademiens Handlingar*, 24 (1898) 1–39.
- [17] G. Blanchard, M. Maunaye, G. Martin, Removal of heavy metals from waters by means of natural zeolites, *Water Res.*, 18 (1984) 1501–1507.
- [18] Z. Zhao, X. Li, Y. Chai, Z. Hua, Y. Xiao, Y. Yang, Adsorption performances and mechanisms of Amidoxime Resin toward Gallium(III) and Vanadium(V) from Bayer Liquor, *ACS Sustainable Chem. Eng.*, 4 (2016) 53–59, <https://doi.org/10.1021/acssuschemeng.5b00307>.
- [19] G.E. Boyd, A.W. Adamson, L.S. Myers Jr., The exchange adsorption of ions from aqueous solutions by organic zeolites. II. Kinetics, *J. Am. Chem. Soc.*, 69 (1947) 2836–2848.
- [20] H. Freundlich, Über die adsorption in lösungen, *Z. Phys. Chem.*, 57 (1906) 385–471.
- [21] H.N. Tran, S.-J. You, A. Hosseini-Bandegharai, H.-P. Chao, Mistakes and inconsistencies regarding adsorption of contaminants from aqueous solutions: a critical review, *Water Res.*, 120 (2017) 88–116.
- [22] G. Socrates, *Infrared and Raman Characteristic Group Frequencies*, John Wiley and Sons, Hoboken, NJ, 2004, <https://doi.org/10.1002/jrs.1238>.
- [23] I. Langmuir, The adsorption of gases on plane surfaces of glass, mica and platinum, *J. Am. Chem. Soc.*, 40 (1918) 1361–1403.